

Alma Mater Studiorum Università di Bologna
Archivio istituzionale della ricerca

Effect of Gold Particles Size over Au/C Catalyst Selectivity in HMF Oxidation Reaction

This is the final peer-reviewed author's accepted manuscript (postprint) of the following publication:

Published Version:

Megias-Sayago C., Lolli A., Bonincontro D., Penkova A., Albonetti S., Cavani F., et al. (2020). Effect of Gold Particles Size over Au/C Catalyst Selectivity in HMF Oxidation Reaction. CHEMCATCHEM, 12(4), 1177-1183 [10.1002/cctc.201901742].

Availability:

This version is available at: <https://hdl.handle.net/11585/787544> since: 2023-04-23

Published:

DOI: <http://doi.org/10.1002/cctc.201901742>

Terms of use:

Some rights reserved. The terms and conditions for the reuse of this version of the manuscript are specified in the publishing policy. For all terms of use and more information see the publisher's website.

This item was downloaded from IRIS Università di Bologna (<https://cris.unibo.it/>).
When citing, please refer to the published version.

(Article begins on next page)

Effect of gold particles size over Au/C catalyst selectivity in HMF oxidation reaction

C. Megías-Sayago^[a], 1, A. Lolli^[b], D. Bonincontro^[b], A. Penkova^[a], S. Albonetti^[b], F. Cavani^[b], J. A. Odriozola^[a] and S. Ivanova^{*[a]}

Abstract: A series of different size gold nanoparticles are prepared, immobilized on activated carbon and applied in the 5-hydroxymethyl furfural (HMF) oxidation to 2,5-furandicarboxylic acid (FDCA) at low base concentration. The variation of the gold particles size influences significantly the product selectivity and carbon balance but not the HMF conversion. The oxygen reduction reaction, thermodynamically favorable over Au (100) face, is judged responsible for this behavior. Au 100/111 exposure ratio is calculated and correlated with gold particle size through the van Hardeveld - Hartog model and related with the observed FDCA selectivity, showing that the alcohol function oxidation is indirectly size dependent.

Introduction

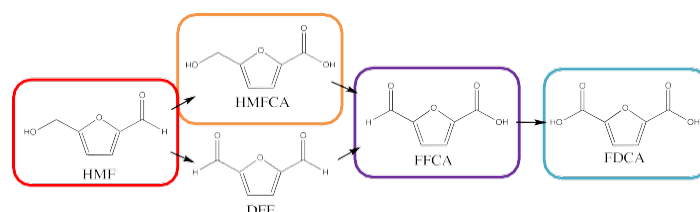
The progressive future substitution of petroleum-based chemicals with sustainable bio-based products passes through the valorization of renewable lignocellulosic biomass in molecules able to replace those employed nowadays. Lignocellulosic components are rich sources of platform chemicals available for dehydration, hydrogenation and/or oxidation reactions in separate or in consecutive manner. 2,5-furandicarboxylic acid (FDCA) is a very good example of such chemical. Its production includes the reactions of biomass depolymerization, hexoses isomerization and dehydration to 5-hydroxymethyl furfural (5-HMF) and its oxidation to the final FDCA product. FDCA is a potential substitute of terephthalic acid, used for polyethylene terephthalate plastics production, because of their structural similarity and final plastics properties likeness [1,2].

5-HMF to FDCA selective oxidation occurs either in homogeneous conditions, using KMnO_4 or metal halides [3–5] or over noble metals based heterogeneous catalysts [6–8]. Within the group of catalytically active noble metals in oxidation reactions, particular interest awakes gold, longtime considered as metal with poor ability to activate oxygen. However, more and more studies confirmed that gold – oxygen interactions are controlled by the

support nature or by the size of the metal clusters [9–11], higher the exposed gold surface to the oxidant higher the overall reaction rate. When the oxidation reactions occur in gas phase the catalyst should activate dioxygen and if the participation of the support material is null (referring to bare or supported gold clusters over non-reducible oxides or carbon) the activation of dioxygen is reported to involve charge transfer from Au to O_2 . As a consequence, the O-O distance increases and superoxo-like state (O_2^-) appears accompanied most probably by partially reduced gold, very difficult to detect as purely cationic state due to important electronic structure rearrangements [12,13].

It is very different when the oxidation occurs in liquid phase; the dissolution of dioxygen and its reaction with the media ought to be taken into consideration. Fristrup et al. [14] studied gold-catalyzed, aerobic oxidation of aldehydes in methanol and found that dioxygen was not directly involved in the oxidation process but indirectly after reacting with the solvent. The same was proposed for aqueous media where dioxygen reacts indirectly as hydroxide ions generator [15]. Those hydroxides participate after in the reactions of aldehydes and alcohols oxidation where the H abstraction of the group to be oxidized is promoted in presence of base.

Referring to HMF oxidation reaction over gold, three oxidation steps are available i) HMF's aldehyde to carboxylic group oxidation giving 5-hydroxymethyl-2-furancarboxylic acid (HMFA) and ii) two step oxidation of the HMFA's OH group to aldehyde, 5-formyl-2-furancarboxylic acid (FFCA), and dicarboxylic acid, 2,5-furan dicarboxylic acid (FDCA). As long as the OH^- are present or generated in the media the HMF oxidation occurs selectively towards the final product (scheme 1).



Scheme 1. Reaction path for HMF oxidation to FDCA.

For all above, it is important to study the size/alcohol (aldehydes) function oxidizing ability using HMF as model molecule. The latter will help us to deduce the mechanism of dioxygen activation over gold and clarify its participation in the reaction. To be sure, that the support properties and gold loading do not alter the results, the same support and similar Au loadings will be used.

[a] Dr. C. Megías-Sayago, Dr. A. Penkova, Prof. J. A. Odriozola and Dr. S. Ivanova

Department: Departamento de Química Inorgánica e Instituto de Ciencia de Materiales de Sevilla

Institution: Universidad de Sevilla-CSIC

Address: Américo Vespucio 49, 41092, Seville, Spain

E-mail: svetlana@icmse.csic.es

[b] Dr. A. Lolli, D. Bonincontro, Prof. S. Albonetti, Prof. F. Cavani

Department Dip. di Chimica Industriale "Toso Montanari",

Institution: Università di Bologna

Address: Viale del Risorgimento, 4, 40136 Bologna BO, Italy

Supporting information for this article is given via a link at the end of the document. ~~((Please delete this text if not appropriate))~~

Results and Discussion

Gold particles synthetic parameters are chosen to obtain a great disparity in size. A part of samples prepared and already reported earlier [16] are selected for this study. Their principal characteristics as gold loading and average particle size are summarized in table 1 and an example of typical preparation is presented in the experimental section.

Table 1. Selected samples, corresponding gold loadings, and particle sizes.

Sample	Au loading, wt. %	Particle size, nm ^[a]
AuC_I	2.3	4.8
AuC_II	2.3	6.6
AuC_III	2.4	8.7
AuC_IV	2.0	15.4
AuC_V	2.1	37.9

^[a] measured by TEM

The catalyst's screening as a function of the gold particle size is presented in Figure 1.

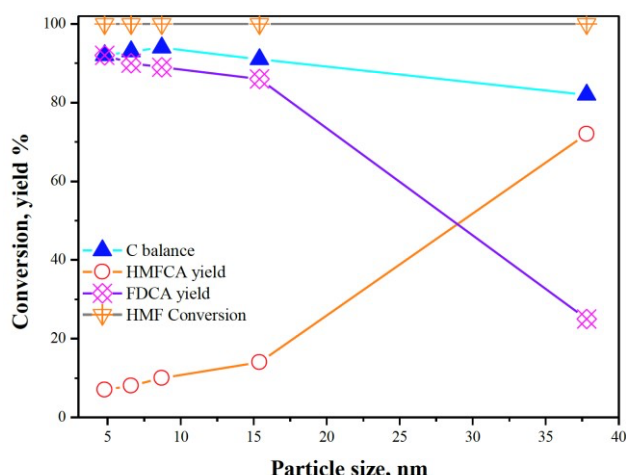


Figure 1. Gold catalysts screening: HMF conversion and HMFCFA, FDCA yields vs. mean particle size. Reaction conditions: HMF: Au: NaOH molar ratio 1:0.01:2, 10 bar O₂, 70 °C, 400 rpm, 4h.

Over gold catalysts, the conversion of HMF to FDCA proceeds through preferential aldehyde group oxidation to HMFCFA and subsequent alcohol group oxidation to FFCA finally transformed into FDCA. Aldehyde group oxidation is a rapid process and normally the FFCA intermediate is absent at the final reaction time. Within the series, no matter the gold particle size, all catalysts present full HMF conversion and only HMFCFA and FDCA are detected as products. On the other hand, the product selectivity and C balance are significantly affected by the particle size. It is interesting to underline that in the 4-16 nm particle size only minor

changes in selectivity are observed disfavoring FDCA for HMFCFA. However, for the particle size superior to 35 nm HMFCFA is the primary product. It seems that aldehyde group oxidation to HMFCFA is less size sensitive than the alcohol group oxidation. There is a decreasing rate of alcohol group oxidation with the particle size, less pronounced in the 4-16 nm size and more evident above that size. So what is making the difference? The conversion is always full so the HMF concentration is not a factor in these conditions. Let's consider the presence of base and oxygen.

It is well known that aldehyde group in basic condition (HMF: OH⁻ of 1:2 in our case) transforms to alkoxide intermediate through nucleophilic addition of hydroxide ion and subsequent proton transfer from water [17,18]. When catalyzed this reaction goes selectively to carboxylic acid but in absence of catalysts Cannizzaro reaction occurs and the aldehyde (HMFCFA) transforms in the corresponding alcohol and carboxylic acid. As for the alcohol oxidation, the OH⁻ groups are reported to participate as H abstractor in the OH group breaking [15,19]. At two base equivalents, as in our case, and considering OH⁻ use in 3 steps the OH⁻ equivalent is not enough for the reaction unless its concentration is continuously renewed. If we reduce the OH⁻ concentration (Figure 2) the HMFCFA is found as major product although FDCA is also found. The presence of both suggests that base is helping in all processes and that the reaction rate of aldehyde oxidation over gold is higher than that of alcohols, the later confirmed also by the absence of the 2,5-Diformylfuran (DFF). It is also interesting to underline that HMF conversion and HMFCFA production are almost equimolar suggesting that the first process is using the starting excess of base before all the other processes and that a full conversion of HMF will be always observed when an initial OH⁻ concentration equal or superior to that of HMF is employed. It should be noted that HMF is not converted in absence of base.

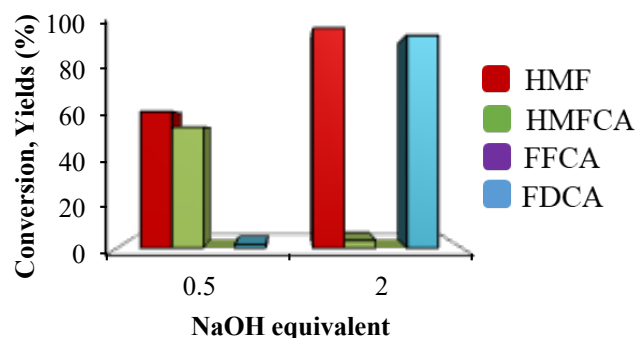
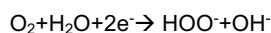


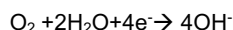
Figure 2. Conversion/yield dependence on base equivalent over AuC_II sample. Reaction conditions: HMF: Au: NaOH molar ratio 1:0.01:0.5 or 1:0.01:2, respectively, 10 bar O₂, 70 °C, 400 rpm, 4h.

At this point, a new charge of OH⁻ is necessary for all other steps. Here is where oxygen enters in the equations. Davis et al. [20] found using labeling experiments that oxygen involved in the

oxidation of alcohols is not incorporated directly from dioxygen but from OH⁻ groups present in the reaction media. They conclude that the role of dioxygen is indirect as regenerator of the hydroxide ions. The only way to generate hydroxides from O₂ in aqueous media is its reduction. Two possible ways of oxygen reduction in alkaline media is generally reported, 2-electron reduction with the formation of peroxide ions



and 4-electron reduction



reaction observed only on Au (100) surfaces and its vicinals. This reaction over gold is of particular interest, as an important size sensitivity is observed, converting Au (100) surfaces in the most active known catalyst for the 4-electron O₂ reduction [21–24]. Although the application of electrochemical potential is generally reported for this reaction, on small gold nanoparticles, *i.e.* with high Au (100) surface exposure and high OH⁻ coverage, the oxygen reduction reaction is thermodynamically favorable. In addition, the oxidation of aldehydes (2-electron oxidation) and that of alcohols (4-electron oxidation) to carboxylic acid assures the necessary electrons.

Considering that gold is an fcc metal and expose (111) and (100) surfaces (Figure 3 inset), every change in its size will produce a change in its (100)/(111) surface ratio. Using the model of van Hardeveld and Hartog [25] one can calculate the surface atoms and sites corresponding to both surfaces and their relation with the experimental average particle size (Figure 3).

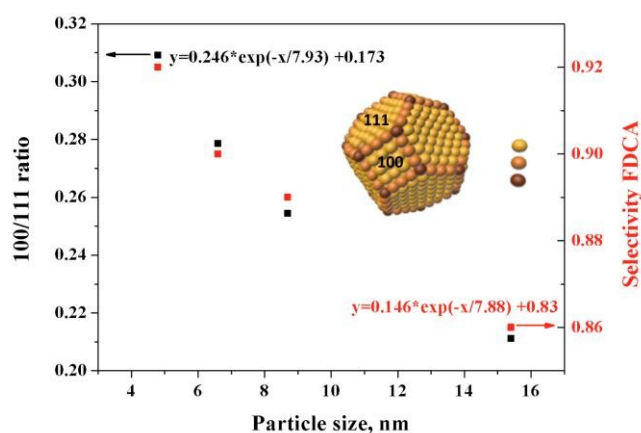


Figure 3 100/111 surface ratio for the studied samples and FDCA selectivity dependence on particle size.

The 100/111 gold surface ratio decreases exponentially with the particles size as well as the FDCA selectivity. Both dependences can be fitted to equation of exponential decay of 1st order. It is interesting, that both equations present a similar exponent coefficient, which suggests that there is a direct relationship

between the processes involved over Au (100) surface and FDCA production. If we consider that at high 100/111 ratio the 4-electron oxygen reduction occurs with hydroxide ions as a product, the oxidation of HMFCA proceeds and the FDCA yield is higher. All processes need base, O₂ reduction and alcohol/aldehyde oxidation. The Au (100) surfaces must be covered by OH⁻ to produce AuOH_{ads} in order to reduce the potential of O₂ to HOO⁻ and to OH⁻ 2nd step reduction [26]. So, for hydroxide ion generation (O₂ activation) over gold we need preferential exposure of the Au (100) face, *i.e.* particles as small as possible and presence of base in order to promote the 4-electrons O₂ reduction and to renew continuously the hydroxide ions concentration required to accomplish the reaction to FDCA. The latter means that at bigger excess of base the reaction more probably is not size sensitive and the oxidation will occur using the hydroxide ions from the media.

To confirm the findings and to see the stability of the catalysts two of the samples are selected AuC_II and AuC_III. Both samples are subjected to 4 cycles of reaction keeping the HMF: Au: NaOH ratio constant (Figure 4). Our previous study over deactivation behavior of those systems [27] in the reaction of glucose to gluconic acid oxidation reveals that a particle size increase occurs after the 1st cycle of the reaction and remain constant till the 4th cycle. The same is detected in this study during the cycles of HMF oxidation. The AuC_II sample size increases from 6.6 to 8.8 nm and that of AuC_III sample increases from 8.7 to 12.2 nm (Figure 5, TEM distribution after the 4th cycle).

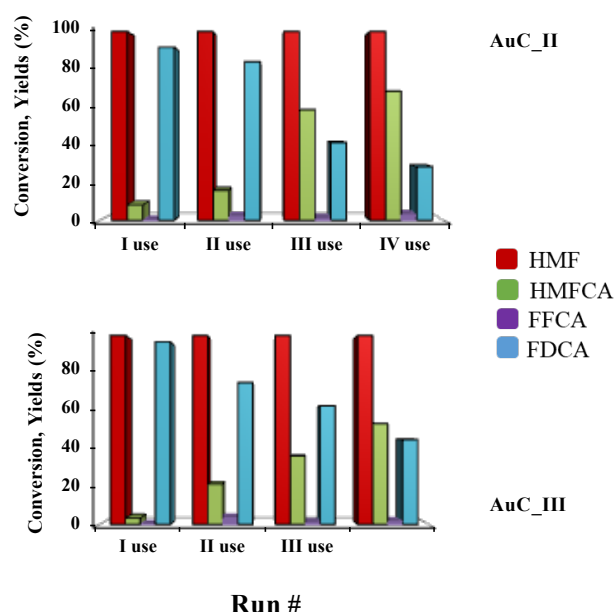


Figure 4. Reuse of AuC_II and AuC_III sample. Reaction conditions: HMF: Au: NaOH molar ratio 1:0.01:0.5 or 1:0.01:2, respectively, 10 bar O₂, 70 °C, 400 rpm, 4h.

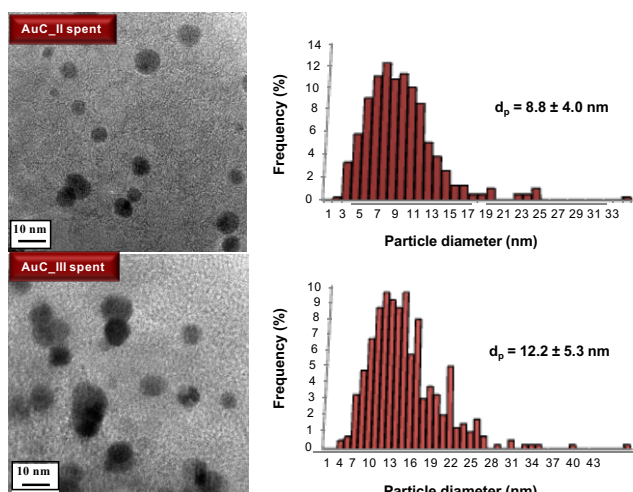


Figure 5. Representative TEM images and gold particle size distributions of AuC_II and AuC_III spent samples after 4 cycles.

If our theory for size dependent O_2 reduction and related FDCA formation is true all cycles after the 1st one should give similar FDCA selectivity to those measured for samples with similar particle size. Actually, it is true for the 2nd run where the FDCA selectivity of the spent AuC_II sample (8.8 nm) is very close to that of fresh AuC_III sample (8.7 nm) (90 vs. 89 %FDCA) and for the spent AuC_III sample (12.2 nm) and fresh AuC_IV sample (15.4 nm) (86 vs. 75 % FDCA). However, in the 3rd and 4th cycle the catalyst continues to lose FDCA selectivity. This change in the oxidation behavior, not caused by the size modification, could be assigned to a continuous change of the symmetry of the Au (100) surface from four-fold to six-fold layers [28]. This change causes decrease in the OH^- adsorption over Au (100) thus inhibiting the 4-electron reduction, *i.e.* Au (100) surface starts to behave as Au (111) surface. Hausen et al. [29] reported that the velocity of reconstruction of the Au (100) surface is higher than that for Au (111). This reorganization, described as network of dislocations, produces important changes on surface' electric potential thus altering its electronic properties and reflecting in negative effect on OH^- adsorption behavior and reactivity. The $AuOH_{ads}$ species concentration decreases together with O_2 reduction reaction rate and FDCA selectivity. It appears that subtle change in particle size affects greatly the O_2 activation behavior of gold and it is much more noticeable for the lower size samples. XPS analysis (Figure 6) also showed an effect on gold particles size dispersion for AuC_I and AuC_V samples, as representatives for the lowest and highest particle size samples. Gold is present as metallic gold before and after the reaction with $4f_{5/2}$ and $4f_{7/2}$ transitions situated at 88.2 and 84.5 eV, respectively. High-resolution XPS oxygen (Figure 7) analysis shows an increase of the oxygen species on the surface after the reaction for both samples with higher concentration of O_2 species found for the bigger size sample. When the difference between the initial and the post reacted spectra is made the bigger particles size catalyst shows a

principal oxygen contributions at ~ 531 eV with a shoulder at ~534 eV, whereas the lower size sample only one contribution at ~532 eV. All contribution can be assigned to sodium carboxylates or esters suggesting the presence of intermediates and/or products on the post reaction catalyst surface [30,31]. The latter is expected as the lowest C-balance is observed for the bigger size particles and suggests that the adsorption/desorption behavior on the surface is also affected by the particle size. Higher the size lower the rate of the reaction and higher the products/intermediates adsorption.

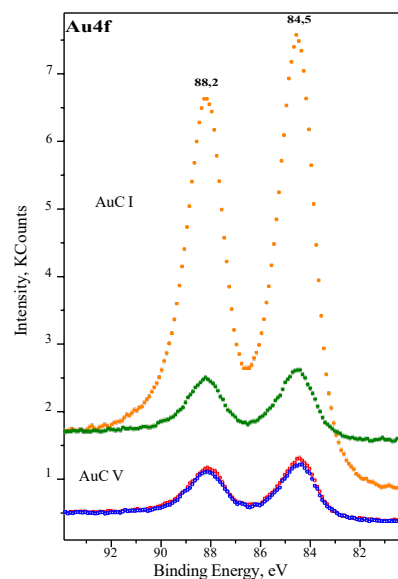


Figure 6. XPS spectra of Au 4f of fresh and spent AuC_I and AuC_V catalysts.

The activity of gold in low base environments is conditioned by the hydroxide ions presence, either added as base or produced via $2e^-$ or $4e^-$ O_2 reduction. This reaction is thermodynamically favorable over low gold particles size where the Au (100) surface exposure is maximal. That surface accelerates the 4-electron oxygen reduction reaction, increases significantly the hydroxide ions concentration, and influences positively the alcohol/aldehyde oxidation rate. It is important to underline that this model applies only for particles within the 4-20 nm range. Bigger particles do not fulfill this relationship and other mechanisms should be applied. The latter is also confirmed by the important change of the C balance for the sample AuC_V. This C-loss is produced either by gold surface covering with intermediates or by Cannizzaro reaction products (although not detected during the analysis).

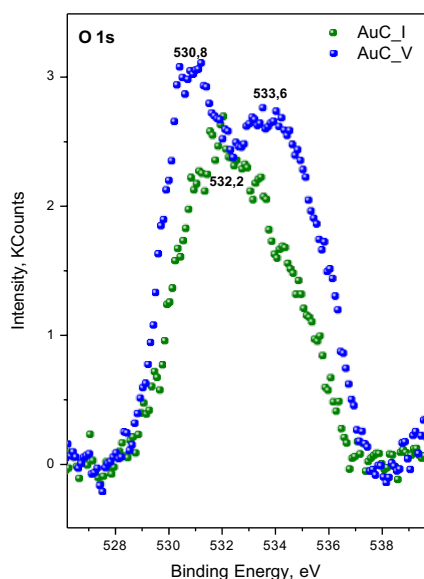


Figure 7. XPS spectra difference of O 1s (spent – fresh sample) for AuC_I and AuC_V catalysts.

Conclusions

Several AuC catalysts differing in metal particle size are prepared and tested in the HMF oxidation to FDCA at low base concentration. No matter the gold particle size, full HMF conversion is achieved in all cases, contrary to the observed products selectivity and C balances. Differences in both are more evident above 16 nm gold particle size, being possible to obtain good performances with slight changes within 4–16 nm range. The obtained results evidence that the alcohol function oxidation is size sensitive, fact that is directly related with the oxygen reduction ability and base concentration. Thermodynamically favorable 4-electron oxygen reduction over Au (100) exposed face is enhanced at small particles sizes where Au 100/111 exposure ratio is maximal. The Au 100/111 exposure ratio and FDCA selectivity correlation reveals an important gold size/structure dependence in the HMFCa to FFCA oxidation at low base concentrations.

Experimental Section

Catalyst series

The samples used in this study are selected from a series of catalysts reported earlier [16] as previously indicated in the manuscript. In a typical preparation, $5 \cdot 10^{-4}$ M aqueous solution of gold precursor HAuCl_4 (Johnson Matthey) is contacted with polyvinyl alcohol (PVA, 1 wt.% aqueous solution), used as stabilizer, during 20 min at 600 rpm (room temperature). Afterwards, the particles were reduced with an appropriate amount of 0.1 M freshly prepared NaBH_4 solution. The preformed colloid (2wt% Au nominal value) is immobilized over commercial activated charcoal Darco®

(Sigma Aldrich, 100 mesh). After ageing during 45 min, the resulting solid was recovered by centrifugation then filtered, dried and calcined in static air at 300°C for 2 h. The use of different Au:PVA: NaBH_4 ratios results in different particle size and that allow us to select a few samples with mean particle size ranging between 4 to 40 nm. Specific Au:PVA: NaBH_4 amounts are presented in our previous contribution [16]. The selected samples, their mean particle size and actual gold loadings are resumed in table 1.

Characterization

The gold contents were estimated through ICP analysis by using Horiba Jobin Yvon spectrometer.

Transmission electron microscopy (TEM/STEM) study on particle size and dispersion of the catalysts was performed on FEI TECNAI F20 operating at 200keV. The average gold particle size was estimated based on surface distribution calculations as shown in equation 1:

$$D [3,2] = \frac{\sum_{i=1}^n D_i^3 v_i}{\sum_{i=1}^n D_i^2 v_i} \quad (1)$$

where D_i is the geometric diameter of the i^{th} particle, and v_i the number of particles with this diameter. For particle size distribution, the total number of measured particles overcomes 200 for every sample.

XPS measurements were carried out on Leybold-Heraeus LHS-1020 instrument coupled with EA200 detector and using non chromatic Mg K α (220W, 11kV, 1253,6 eV). Prior to use the sample were pressed into a thin disk. The XPS spectra were recorded at room temperature and the binding energy was calibrated on C1s at 284,6 eV with an uncertainty ± 0.2 eV. The spectra were recorded with constant pass energy of 44 eV and 0.1 eV resolution for the studied zones.

Catalytic tests

The oxidation of HMF was carried out in a 100 mL volume autoclave reactor, provided with mechanical stirrer and temperature/pressure controllers. In a typical experiment, the reactor was charged with an aqueous solution of HMF (approx. 25 mL, 0.08 M), the necessary amount of NaOH, and the catalyst in the HMF: Au: NaOH ratio of 1:0.01:2. Before the test, the reactor was purged twice with pure O_2 (10 bar) and finally pressurized to 10 bars. Temperature was raised to 70°C and the reaction mixture was stirred at approximately 400 rpm for 4 hours. Then the reactor was introduced into an ice bath and the reaction mixture was centrifuged and filtered. Afterwards, a sample was taken and diluted before the test in an Agilent Infinity 1260 liquid chromatograph equipped with a DAD detector and an Aminex HPX-87H 300 mm \times 7.8 mm column using 0.005 M H_2SO_4 as eluent. The stability was studied in the spent samples recovered from the post-reaction mixture and dried at 120°C overnight. HMF: Au: NaOH molar ratios were always kept constant. Conversion, selectivity and yields are calculated after calibration using as reference commercial samples, according to the following equations:

$$\text{Conversion (\%)} = \frac{[\text{HMF}]_F - [\text{HMF}]_I}{[\text{HMF}]_F} \times 100 \quad (2)$$

$$\text{FDCA Selectivity (\%)} = \frac{\text{FDCA mols}}{\text{HMF mols}_I - \text{HMF mols}_F} \times 100 \quad (3)$$

$$\text{FDCA Yield (\%)} = \frac{\text{Conversion}}{100} \times \text{Selectivity} \quad (4)$$

Acknowledgements

Financial support has been obtained from the Spanish Ministerio de Ciencia, Innovación y Universidades (ENE2017-82451-C3-3-R) co-financed by E.U. FEDER funds.

Keywords: HMF oxidation, 2,5-furandicarboxylic acid, gold catalysts, size/selectivity dependence

References

- [1] A. Gandini, A. J. D. Silvestre, C. P. Neto, A. F. Sousa, M. Gomes, J. Polymer Sci.: A: Polymer Chem., 2009, 47, 295–298;
- [2] M. Gomes, A. Gandini, A. J. D. Silvestre, B. Reis, J. Polymer Sci.: A: Polymer Chem., 2011, 49, 3759–3768
- [3] W. Partenheimer, V. V. Grushin, Adv. Synth. Catal. 2001, 343, 102–111.
- [4] L. Ardemani, G. Cibir, A. J. Dent, M. A. Isaacs, G. Kyriakou, A. F. Lee, C. M. A. Parlett, S. A. Parryb, K. Wilson Chem. Sci, 2015, 6, 4940–4945.
- [5] A.S. Amarasekara, D. Green, E. McMillan, Catal. Commun., 2008, 9, 286–288.
- [6] S. E. Davis, L. R. Houk, E. C. Tamargo, A. K. Datye, R. J. Davis, Catal. Today, 2011, 160, 55–60.
- [7] M. Ventura, A. Dibenedetto, M. Aresta, Inorg. Chim. Acta, 2018, 470, 11–21.
- [8] S. Albonetti, A. Lolli, V. Morandi, A. Migliori, C. Lucarelli, F. Cavani, Appl. Catal. B: Environm., 2015, 163, 520–530.
- [9] M. Boronat, A. Corma, Dalton Trans., 2010, 39, 8538–8546.
- [10] N. López, J. K. Nørskov, J. Am. Chem. Soc., 2002, 124, 11262–11263.
- [11] T. Jiang, D. J. Mowbray, S. Dobrin, H. Falsig, B. Hvolbæk, T. Bligaard, J. K. Nørskov, J. Phys. Chem. C, 2009, 113, 10548–10553.
- [12] J.A. van Bokhoven, C. Louis, J. T. Miller, M. Tromp, O. V. Safonova, P. Glatzel, Angew. Chem. Int. Ed., 2006, 45, 4651–4654.
- [13] A.P. Woodham, G. Meijer, A. Fielicke, J. Am. Chem. Soc., 2013, 135, 1727–1730.
- [14] P. Fristrup, L. Bahn Johansen, C.H. Christensen, Chem. Commun., 2008, 2750–2752
- [15] B. N. Zope, D. D. Hibbitts, M. Neurock, R. J. Davis, Science, 2010, 330, 74.
- [16] C. Megías-Sayago, J.L. Santos, F. Ammari, M. Chenouf, S. Ivanova, M.A. Centeno, J.A. Odriozola, Catal. Today, 2018, 306, 183–190.
- [17] K.P.C. Vollhardt, N.E. Schore Organic Chemistry 2nd Ed., W.H. Freeman and Company
- [18] S. Warren, Chemistry of the carbonyl group: a programmed approach to organic reaction mechanisms. Wiley, 1974.
- [19] C. Shang, Z.-P. Liu, J. Am. Chem. Soc., 2011, 133, 9938–9947.
- [20] S. E. Davis, B. N. Zope, R. J. Davis, Green Chem., 2012, 14, 143–147.
- [21] R.R. Adzic, N.M. Markovic, J. Electroanal. Chem., 1982, 138, 443–447.
- [22] R.R. Adzic, N.M. Markovic, V. B. Vesovic, J. Electroanal. Chem., 1984, 165, 105–120.
- [23] R.R. Adzic, N.M. Markovic, V. B. Vesovic, J. Electroanal. Chem., 1984, 165, 121–133.
- [24] N. M. Markovic, I. M. Tidswell, P. N. Ross, Langmuir, 1994, 10, 1–4.
- [25] R. van Hardeveld, F. Hartog, Surface Science, 1969, 15, 189–230.
- [26] P. Fischer, J. Heitbaum, J. Electroanal. Chem., 1980, 112, 231–238.
- [27] C. Megías-Sayago, L.F. Bobadilla, S. Ivanova, A. Penkova, M.A. Centeno, J.A. Odriozola, Catal. Today, 2018, 301, 72–77.
- [28] S. Strbac, R.R. Adzic, J. Electroanal. Chem., 1996, 403, 169–181.
- [29] F. Hausen, J.A. Zimmet, R. Bennewitz, Surface Science, 2013, 607, 20–24.
- [30] C.D. Wagner, D.A. Zatko, R.H. Raymond, Anal. Chem. **1980**, 52, 1445–1451
- [31] G.P. Lopez, D.G. Castner, B.D. Ratner, Surf. Interface Anal., **1991**, 17, 267–272.